

Effect of holes and stiffeners on the behavior of Eccentric loaded cold-formed steel built-up channel columns - numerical investigation

Ziqi He¹, Guang Yang², Ben Schafer³, Xuhong Zhou⁴

Abstract

Cold-formed steel members often need to be opened in the web due to the passage of the building system pipeline. In general stiffeners of the web maybe strengthen their structural performance. In the field of cold-formed steel structures, such as multi-layer houses, wall frames and portal frames, the use of built-up cold-formed steel channel sections are becoming increasingly popular. Such members are often under the combined effects of compression and bending. Limited research has been done on the subject. In this paper, the back-to-back built-up cold-formed steel beam-columns are studied to understand the influence of stiffeners and openings on the ultimate bearing capacity and failure mode. First, this paper presents the results of experimental tests performed on back-to-back built-up cold-formed steel channel sections under axis and eccentric compression. Detailed observations on different failure modes and column strengths were made through varying the location of stiffeners and holes, length and cross section of columns, the magnitude and direction of eccentricity. Then, a non-linear finite element model was developed which includes material non-linearity, geometric imperfections and explicit modeling of web fasteners. A comprehensive parametric study consisting of 222 models has been carried out covering a wide range of eccentricity and web fasteners for the considered back-to-back built-up columns. Finally, based results of numerical research, the ultimate capacities were used to assess the performance of the current technical specifications of cold-formed thin-walled steel structures, North American codes, AS/NZS and China specification. As the test cannot be done during the epidemic, the correctness of the formula needs to be verified by subsequent tests.

I. Introduction

Scholars at home and abroad have conducted a lot of research on cold-formed thin-walled steel, from single-leg to multi-leg, from simple C and Z-shaped cross-sections to Σ , I-shaped cross-sections, and from web openings to single-hole or porous. As mentioned earlier, the split section and web stiffening are to increase the bearing capacity of the components, and the web opening is to facilitate the installation of the pipeline. At present, there is little research on the split section with web stiffening and openings at home and abroad, and the following should be paid attention to: (1) The research of domestic and foreign scholars is mostly concentrated on axial compression, and there are few researches on compression and bending. (2) Stiffening, splicing, and opening are important ways to increase the bearing capacity and improve the use of cold-

formed components. The impact is very valuable and necessary for research and should be considered comprehensively. (3) At present, there is no direct strength method calculation formula for the split section, and a more effective direct strength method formula can be put forward using experiments and finite element analysis.

This paper introduces the finite element analysis and research of split H-shaped compression-bending members based on C-section and Σ -section. The length, number of openings and the spacing of fasteners are changed. The results of the finite element analysis were compared with the current Chinese and American standards, and suggestions for improvement were put forward.

II. Finite Element Model

In this paper, ABAQUS (2016) finite element software is used for modeling and analysis, and the compression-bending components, fastening screws, short plates, etc.

are modeled, and the buckling mode and failure load of the specimen are obtained through finite element simulation.

2.1 Specimen parameters

In this study, there are two types of compression-bending components, one is based on a split H-section with a C-shaped section with one-folded edge, and the other is a split H-section based on a Σ -section. Each section has four lengths: 400mm, 1000mm, 1600mm, and 2200mm. For the 400mm long model, do not open holes, take the screw spacing of 100mm and 300mm; for a 1000mm long model, open a hole and take the screw spacing of 150mm, 450mm, and 900mm; for a 1600mm long model, open a hole and take the screw spacing of 300mm, 750mm, 1500mm; for the 2200mm long model,

open two holes and take the screw spacing of 300mm, 700mm, 1050mm. The cross-sectional dimensions are shown in Figure 1 and Figure 2, and the cross-sectional characteristics are listed in Table 1.

In the finite element model, all CFS (cold-formed steel) composite section components are modeled using a common 4-point shell element (S4R), and each node has six degrees of freedom (three translations and three rotations). S4R can simulate the behavior of thin, thick and double-bent shells. The limbs of the compression-bending parts are connected by simulated screws. The screw cap adopts a three-degree-of-freedom 8-node solid element and the screw adopts a beam element.

Table 1 Sectional characteristics

section	h(mm)	b(mm)	c(mm)	t(mm)	A(mm ²)	I _x (mm ⁴)	I _y (mm ⁴)	W _x (mm ³)	W _y (mm ³)	f _y (Mpa)
C-section split	120	80	20	2	1313.14	3306498.9	2463184.7	55108.3	30789.8	345
Σ -section split	120	80	20	2	1325.66	3209881.9	2425632.9	53498	30320.4	345

Each end of the bending part is connected with an end plate, and the end plate uses R3D4 discrete rigid unit. Figure 4 shows some of these finite element models.

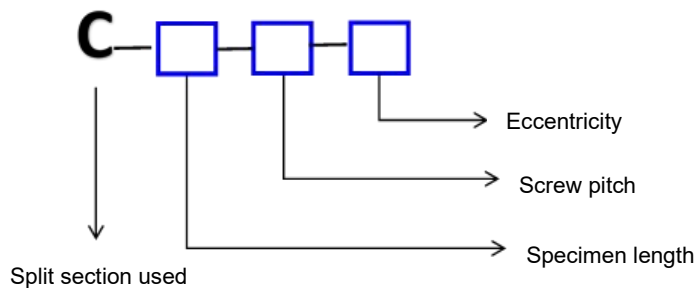


Figure 1 Numbering rules of test pieces

2.2 Geometric model and material properties

In this simulation, three types of parts were created: pressure parts (C-shaped section and Σ -shaped section), screws, and end plates. Among them, the constitutive model of the compression component material adopts a bilinear model, the yield strength is 345 MPa, the elastic modulus is 2.15×10^5 MPa, and the Poisson's ratio is 0.3.

In the interaction, the contact surface of the split part uses a frictionless, "hard" contact surface-to-surface contact type. The contact surface of the screw and the pressure part is defined as TIE constraint, and the end plate is connected with the pressure part by TIE constraint. MPC restraint is used between the screw and the nut to apply bolt load.

2.3 Boundary conditions and loading methods

The boundary condition of hinged on both sides is adopted, and the torsion of the bar around the longitudinal axis is restrained. In the nonlinear analysis, three analysis steps are defined. The first two analysis steps are to apply the initial bolt force, and the third analysis step is to use the riks method to find the bearing capacity of the member. By referring to the self-tapping screws for the structure, the bolt pre-tightening force is 5kN. When the riks method is used to obtain the bearing capacity of the bar,

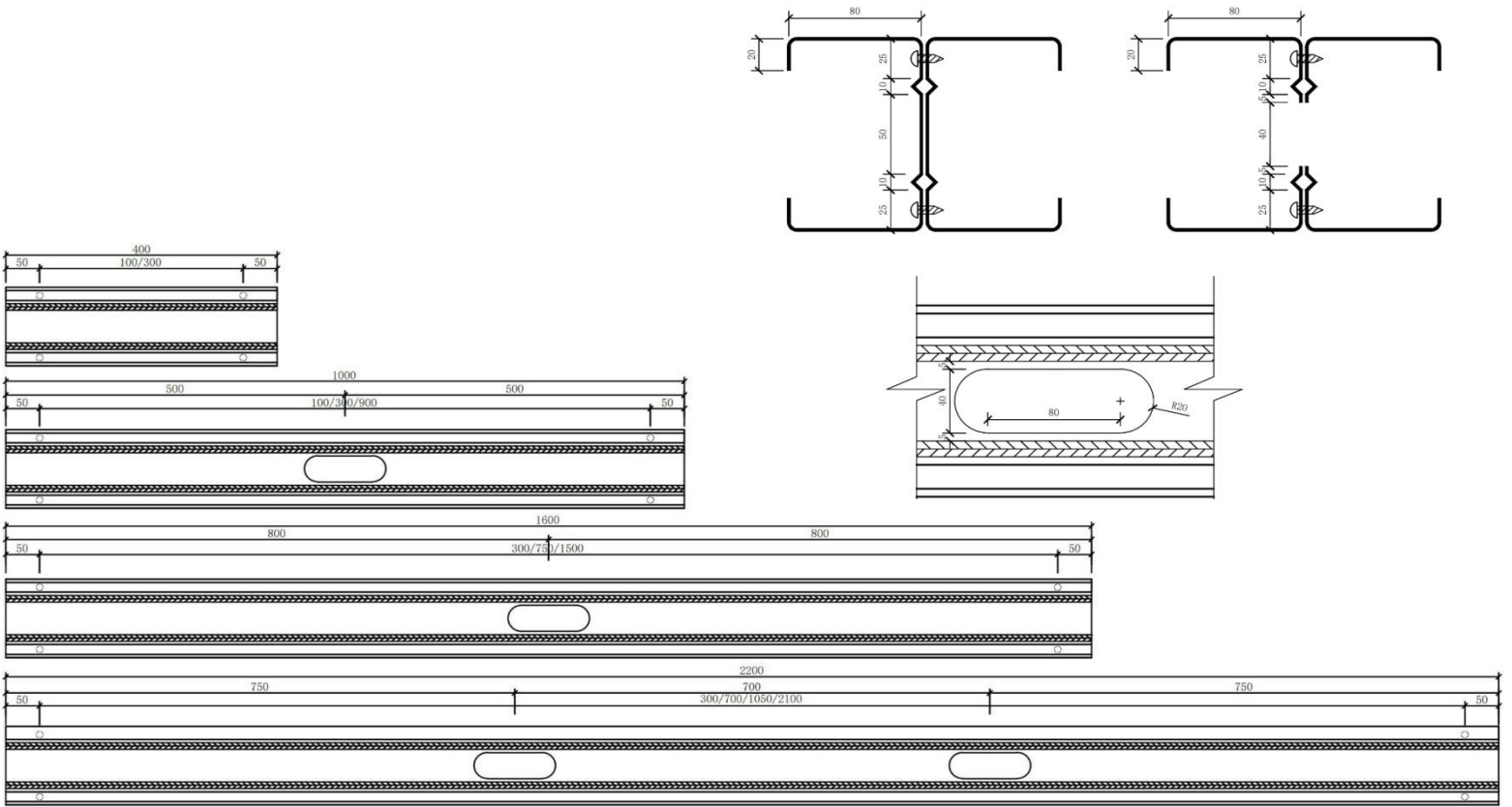


Figure 2 C-shaped cross-section split H-shaped bending member

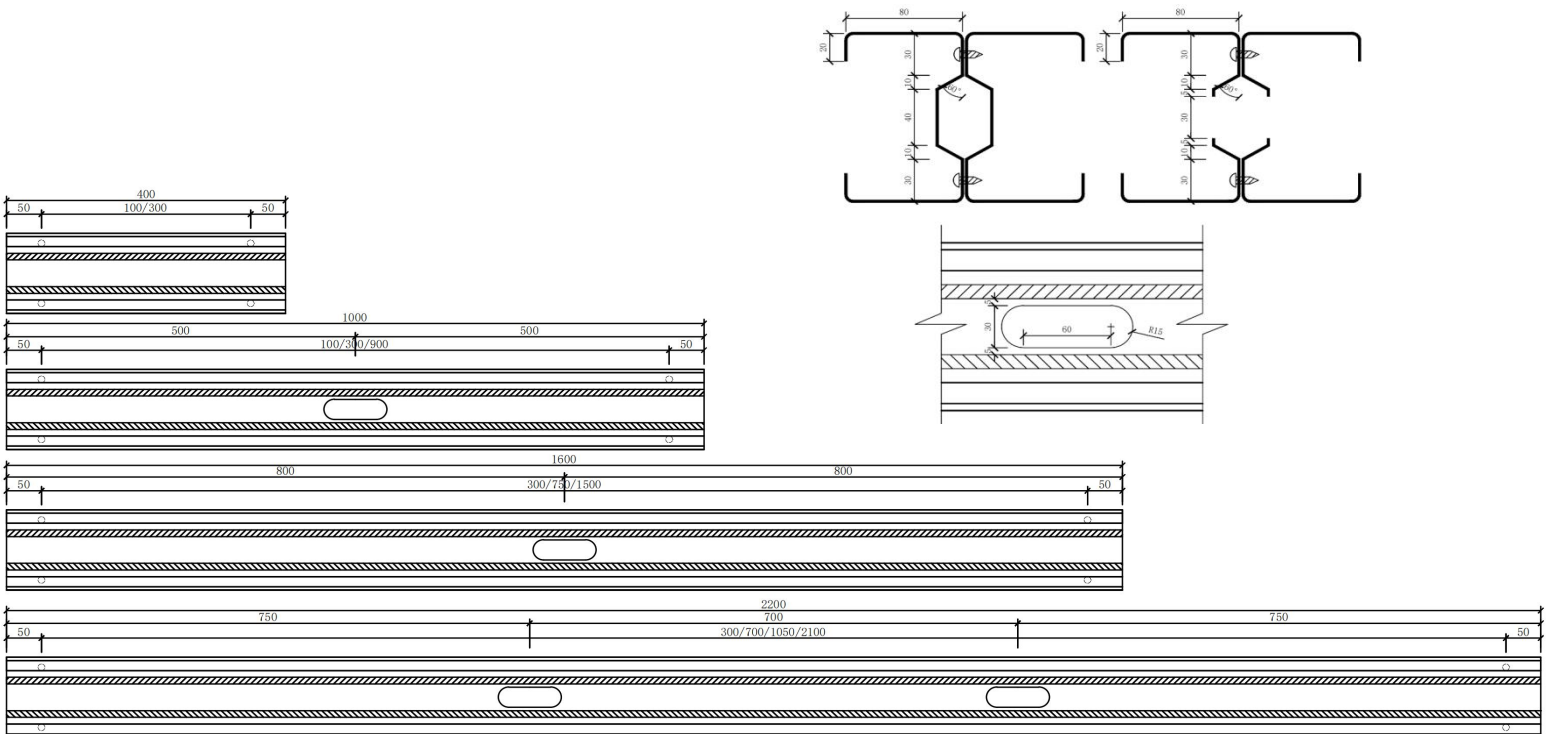


Figure 3 Σ -shaped section split H-shaped bending member

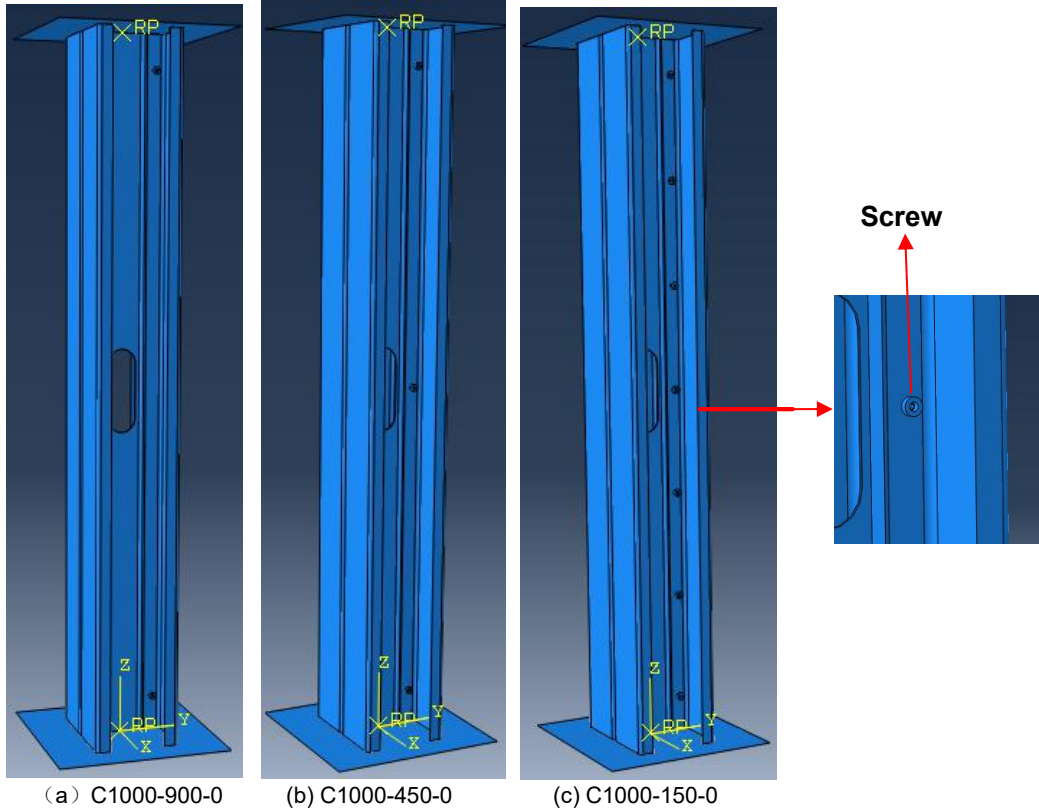


Figure 4 Part of the finite element mode

displacement loading mode is used to facilitate the post-processing to obtain the maximum bearing capacity.

2.4 Simulation of initial defects

Through some literature reading, the influence of residual stress is ignored this time. For geometric defects, the imperfection command in ABAQUS is used to simulate. This method has achieved great success in previous studies. First, in ABAQUS, the advanced BULKLE buckling analysis is used to obtain the buckling mode, and then the first mode of the buckling analysis is used to perform the nonlinear analysis of the compression member using the imperfection command.

2.5 Parameter analysis

A total of 222 nonlinear finite element models were analyzed this time, dedicated to the study of the bending performance of cold-formed split bars and the influence of screws on the split bars. The analysis results are shown in Table 2. It can be seen from the result table that as the eccentricity increases, the bearing capacity of the rods

decreases; with the increase of the screw pitch, the bearing capacity generally shows a downward trend, but there are also counterexamples.

III. Comparison with specifications and the proposal of direct strength method

3.1 Comparison with current regulations

At present, the Chinese standard GB50018-2002 "Technical Design Specification for Cold-Formed Thin-Walled Steel Structures" calculates the bearing capacity of bending members as follows:

$$\frac{N}{\varphi A_e} + \frac{\beta_m M}{(1 - \frac{N}{N_E}) W_e} \leq f$$

The design value of the bearing capacity of the member can be obtained by bringing $M=Ne$ into it. This method requires iterative calculation. However, the specification does not propose a design method for compression-bending members with holes. The standard formula is now used to calculate the bearing capacity of the members in

this study, without considering the effect of holes. The standard formula is now used to calculate the bearing capacity of the members in this study, without considering the effect of holes. In order to simplify the calculation, replace the N in the next step $(1 - \frac{N}{N_E})$ with the bearing capacity N calculated in the previous step, that is, first calculate the axial load bearing capacity N_0 , replace N_0 with the N in the numerator $(1 - \frac{N}{N_E})$ of the $e=s5$ formula, and so on.. The value of $E400-100-s5$ calculated by this method is 397342.9N, the accurate value is 399089.9N, the error is 0.4%, which is slightly smaller than the accurate value.

Table 3 is the comparison between the finite element results and the Chinese standard calculation results. The value in the table is the ratio of the standard calculation value and the finite element calculation value. It can be seen from Table 4 that when the eccentricity is less than 30mm, the value calculated by the specification is almost larger than the value of the finite element. Considering the simplified calculation method, the actual specification value is even larger. With the increase of the eccentricity, the standard value gradually changes from the initial value larger than the finite element calculation value to close to or smaller than the finite element calculation value. When considering the influence of holes, the standard formula can be revised. Since the contribution of the web to the resisting bending moment is relatively small, the former part $(\frac{N}{\varphi A_e})$ of the formula can be revised, such as multiplying the formula by a number greater than 1, the magnitude of this value depends on the number of holes and the ratio of the hole diameter to the height of the web.

3.2 Suggested direct strength method formula

At present, the effective section method is generally used in the code to calculate the ultimate bearing capacity of members. This method needs to calculate the effective cross-sectional area and effective cross-sectional modulus.

As the cross-sectional form becomes more complicated, the calculation is more difficult, and the method is based on the influence of the local buckling of the plate on the bearing capacity of the member, and the distortion buckling performance of the member cannot be considered. In order to make up for the shortcomings of the effective section method, the direct strength method that uses full section to calculate the ultimate bearing capacity of members has attracted more and more attention from researchers. At present, the research results of the direct strength method are only applicable to simply supported members under axial compression or pure bending. As the force of eccentric compression members is more complicated, the application research results of this method in eccentric compression members are still relatively scarce. Given that it is still difficult to directly establish the direct strength method formula for biased members, the idea of finding the P-M relationship for biased members in general steel is used for reference. Based on the direct strength method formula of axial compression or pure bending members, a P-M relationship suitable for cold-formed thin-walled steel biased members is proposed [22].

Based on the results of this finite element analysis, when the failure mode dominated by local instability occurs, the relationship between P/P_{nl} and M/M_{nl} is shown in Figure 5.

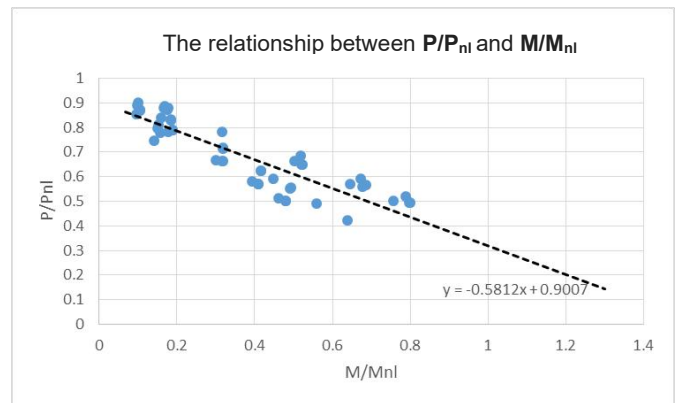


Figure 5 The relationship between P/P_{nl} and M/M_{nl}

When $0 < P/P_{nl} \leq 1$,

$$\frac{P}{P_{nl}} = -0.58 \frac{M}{M_{nl}} + 0.9$$

When the specimen has a failure mode dominated by distortional buckling, the relationship between P/P_{nd} and M/M_{nd} is shown in Figure 6.

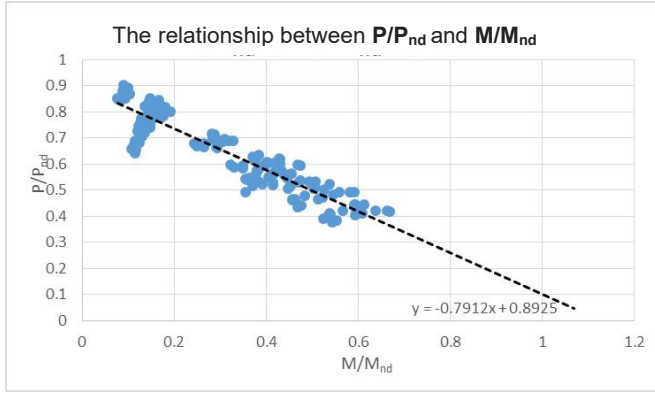


Figure 6 The relationship between P/P_{nd} and M/M_{nd}

When $0 < M/M_{nd} \leq 1$,

$$\frac{P}{P_{nd}} = -0.79 \frac{M}{M_{nd}} + 0.89$$

In the formula: P_{nl} and P_{nd} are the ultimate bearing capacity corresponding to the partial instability and distortional instability of the member under axial compression obtained according to the calculation formula of the direct strength method specified in the North American (Canada) code (North American specification for the design of cold-formed steel structural members (S136-12)). M_{nl} and M_{nd} are the ultimate bearing bending moments corresponding to the partial instability and distortional instability of the member in the purely bending state.

As the test cannot be done during the epidemic, the correctness of the formula needs to be verified by subsequent tests.

IV. Conclusion

This article describes the analysis of the buckling mode and bearing capacity of 400mm, 1000mm, 1600mm, 2200mm long bore compression-bending specimens using ABAQUS finite element software. During the simulation, the screw pitch of the test piece was also changed to explore

the influence of the screw pitch on the bearing capacity. The results show that: the members mainly have local buckling and distortional buckling; as the eccentricity increases, the bearing capacity of the members decreases; with the increase of the screw spacing, the bearing capacity generally shows a downward trend, but there are also counterexamples. It can be seen that the smaller the pitch is, the bearing capacity of the rod may not necessarily increase, and the appropriate pitch should be selected.

This paper also compares the finite element calculation results with the current Chinese standards and finds that the results of the two are similar, but the specification value is greater than the finite element calculation value within a certain range. The calculation formula can be modified according to the characteristics of the hole (size, number, etc.) In addition, this article also draws on the idea of finding the P-M relationship for biased members in general steel, based on the direct strength method formula of axial compression or pure bending members, and proposes the P-M relationship for cold-formed thin-walled steel split biased members. A suggested formula is proposed, but it needs to be verified by subsequent experiments.

References

- [1] Moen C D, Schafer B W. Elastic buckling of cold-formed steel columns and beams with holes[J]. Engineering Structure, 2009, 31(12): 2812 – 2824.
- [2] Moen C D, Schafer B W. Direct strength design of cold-formed steel columns with holes[C]. 2010 Annual Technical Session and Meeting, Structural Stability Research Council, Orlando, FL. 2010.
- [3] Moen C D, Schafer B W. Direct strength method for design of cold-formed steel columns with holes[J]. Journal of Structural Engineering, ASCE. 2011, 137(5): 559 – 570.
- [4] Moen C D. Direct strength design for cold-formed steel members with perforations[D]. Johns Hopkins University, Baltimore, 2008.

[5] Baokang He, Tianhua Zhou. The unified rule for calculation of the effective width of the cold-formed steel section and the effective width of the AISI standard[J]. Progress in building steel structures (Chinese), 2005, 7(4): 6-10.

[6] Jinjiang Zhou, Shaofeng Yu. The equivalent modulus method calculates the buckling stress of cold-formed thin-walled channel steel columns with holes[J]. Steel structure, 2010, 25(2): 27-31.

[7] Yu Chen. Research on the performance of cold-formed thin-walled crimped channel compression members with web openings[D]. Harbin: Harbin Institute of Technology (Chinese), 2004.

[8] Wen Shuangling. Bending-torsional buckling of cold-formed thin-walled C-section steel columns under axial compression[J]. China Civil Engineering Journal (Chinese), 1996, 29(1): 72-79.

[9] Yonghong Yao, Zhenyu Wu, Bo Cheng, etc. Experimental study on the axial compression performance of cold-formed thin-walled crimped channel steel columns with openings[J]. Journal of South China University of Technology: Natural Science Edition (Chinese), 2011, 39(9): 61-67.

[10] Mingming Liu, Hongying Jiang. Study on seismic performance of beam-column joints with stiffeners at web openings[J]. Steel Construction, 11:7-15.

[11] Min Rao, Xiuwen Yuan, Cheng Zhang. Finite element analysis of cold-formed thin-walled C-shaped steel impure bending members with web openings[J]. Shanxi Architecture (Chinese), 2018, 44(18): 40-41

[12] Zheng Tan, Xingyou Yao, Yang Wang. Experimental Research on Distortional Buckling Bearing Capacity of Cold-formed Thin-walled Steel Axial Compression Members with Openings on the Web[J]. Journal of Nanchang Institute of Technology (Chinese), 2015, 34(6): 14-18

[13] Chungang Wang, Zhuangnan Zhang, Daqian Zhao, Yufei Cao. Axial compression bearing capacity test of Σ -shaped complex crimped channel steel with web openings[J]. Journal of Jilin University: Engineering Edition (Chinese), 2015, 45(3): 788-796

[14] Mohaned, G. (2017). "Axial load capacity of cold-formed steel built-up stub columns." International Journal of Steel Structures, 17(4): 1273-1283 (2017)

[15] Jia-Hui, Zhang, Ben, Young. "Experimental investigation of cold-formed steel built-up closed section columns with web stiffeners." Journal of Constructional Steel Research 147(2018): 380-392

[16] Krishanu Roy, Tina Chui Huon Ting, et. "Experimental and numerical investigation into the behaviour of face-to-face built-up cold-formed steel channel sections under compression." Structures 16(2018): 327-346

[17] Liping Wang, Ben Young. Beam tests of cold-formed steel built-up sections with web perforations[J]. Journal of Constructional Steel Research, 115 (2015): 18-33

[18] Fangfang Liao, Hanheng Wu, Ruizhi Wang, Tianhua Zhou. Compression test and analysis of multi-limbs built-up cold-formed steel stub columns[J]. Journal of Constructional Steel Research, 128 (2017): 405-415

[19] Liping Wang, Ben Young, M. ASCE. Behavior of Cold-Formed Steel Built-Up Sections with Intermediate Stiffeners under Bending. I: Tests and Numerical Validation[J]. Journal of Structural Engineering, 2016, 142(3): 1-9

[20] Liping Wang, Ben Young, M. ASCE. Behavior of Cold-Formed Steel Built-Up Sections with Intermediate Stiffeners under Bending. II: Parametric Study and Design[J]. Journal of Structural Engineering, 2016, 142(3): 1-11

[21] Jia-Hui Zhang, Ben Young. Finite element analysis and design of cold-formed steel built-up closed section columns with web stiffeners[J]. Thin-Walled Structures, 2018, 131: 22-237

[22] Rui Cheng, Songsong Liu, Zongming Huang, Yu Shi, Jia Cui, Zhegang Li. Ultimate bearing capacity of cold-formed thin-walled C-shaped steel eccentric compression members around strong shaft[J]. Chinese Journal of Civil and Environmental Engineering (Chinese), 2018, 40(1): 9-16

Table 2 Finite element analysis results

Specimen number	Buckling mode	P_{FE} (N)										
		e=0mm	e=s5m	e=s10m	e=s20m	e=s30m	e=s40m	e=w5m	e=w10	e=w20	e=w30	e=w40
E400-100	Local	412298	368383	333255	279881	241021	211700	371010	330354	273602	239237	209140
E400-300	Local	410789	366664	332171	278808	240062	210830	366897	328015	272764	236304	208504
E1000-150	Local	369715	338772	310131	264000	229680	202713	332468	294856	234338	194775	167163
E1000-450	distortional	388244	362914	335565	288275	251197	222373	349880	310030	248408	206021	174726
E1000-900	distortional	380824	357282	329961	283609	247523	219255	347057	308556	245177	202905	173035
E1600-300	distortional	379725	348791	318877	271265	236168	209190	327007	284544	226500	190327	166619
E1600-750	distortional	369782	344831	315642	268755	233802	206999	312479	272556	217979	182305	159425
E1600-1500	distortional	366125	341257	313108	264034	232730	206268	311325	271412	217574	181992	158645

E2200-300	distortional	351731	327929	297215	250125	216378	191070	294708	257285	207766	175562	152651
E2200-700	distortional	330056	311887	285556	243681	212512	188629	270134	234745	188671	159280	138479
E2200-1050	distortional	337400	313075	286585	243884	211591	187059	277808	240204	180879	162196	141113
C400-100	Local	384336	358267	333883	287486	250970	222215	356272	325774	275583	237844	209164
C400-300	Local	384802	361283	334501	287483	250908	222282	353017	319310	266310	228675	200784
C1000-150	distortional	345252	321246	297221	257389	226483	201877	311968	277983	227329	190535	162479
C1000-450	distortional	344208	320629	296838	257332	226436	201879	310463	275351	228368	185947	158208
C1000-900	distortional	316633	307668	289259	254477	227236	202206	276678	242977	197504	164020	139456
C1600-300	distortional	308383	295951	273618	235760	206739	183886	270174	239037	195339	166406	146307
C1600-750	distortional	332066	309992	285434	245340	215008	191348	282350	249221	203998	174206	152883
C1600-1500	distortional	322290	303559	281649	244451	214857	191419	281241	249175	202977	172893	152465
C2200-300	distortional	304606	286085	262512	225526	198117	176753	257242	225781	183459	156265	137249
C2200-700	distortional	304589	287410	264172	226876	199061	177496	262623	229089	185336	157505	137978
C2200-1050	distortional	289449	279732	258182	223174	196230	175005	245479	216074	177738	152908	134878

Table 3 Comparison of standard calculation value and finite element calculation value

Specimen number	e=0	e=s5	e=s10	e=s20	e=s30	e=s40	e=w5	e=w10	e=w20	e=w30	e=w40
E400-100	1.07822	1.07861	1.075184	1.070004	1.06727	1.064891	0.985475	0.939885	0.871917	0.809593	0.779478
E400-300	1.08218	1.08367	1.078693	1.074122	1.071533	1.069286	0.996522	0.946587	0.874596	0.819642	0.781856
E1000-150	1.14921	1.12696	1.108033	1.08486	1.068934	1.059823	1.044914	0.996486	0.958245	0.932947	0.912897
E1000-450	1.09437	1.05199	1.02405	0.993506	0.977372	0.966124	0.992913	0.947715	0.90397	0.882021	0.873382
E1000-900	1.11569	1.06857	1.041443	1.009852	0.991879	0.979863	1.000989	0.952242	0.915882	0.895566	0.881917
E1600-300	1.05508	1.03812	1.017113	0.989327	0.969128	0.953758	0.987698	0.950799	0.901666	0.861788	0.82249
E1600-750	1.08345	1.05004	1.027537	0.998567	0.978935	0.963853	1.033619	0.992619	0.936913	0.89971	0.859604
E1600-1500	1.09427	1.06104	1.035853	1.016422	0.983445	0.967269	1.03745	0.996803	0.938657	0.901257	0.863831
E2200-300	1.06884	1.03694	1.016709	0.988089	0.966219	0.948123	1.003045	0.946645	0.86697	0.814007	0.775867
E2200-700	1.13903	1.09027	1.05822	1.014218	0.983796	0.960393	1.094292	1.037541	0.954714	0.897217	0.85527
E2200-1050	1.11424	1.08614	1.054421	1.013374	0.988079	0.968454	1.064063	1.013961	0.995842	0.881086	0.839306
C400-100	1.14692	1.10442	1.07235	1.046347	1.03341	1.025771	1.021929	0.951926	0.867964	0.818508	0.784694
C400-300	1.14553	1.0952	1.070369	1.046358	1.033665	1.025461	1.031352	0.971197	0.898187	0.851327	0.817444
C1000-150	1.22033	1.18388	1.155972	1.11873	1.094223	1.07745	1.109431	1.056465	0.991492	0.959792	0.946892
C1000-450	1.22403	1.18616	1.157463	1.118978	1.09445	1.077439	1.114809	1.066564	0.986981	0.983474	0.972455
C1000-900	1.33063	1.23613	1.18779	1.131532	1.090597	1.075696	1.250938	1.208672	1.141216	1.11495	1.103216
C1600-300	1.28984	1.22081	1.187566	1.147332	1.120625	1.10178	1.193184	1.133714	1.05205	0.994602	0.94693
C1600-750	1.19784	1.16551	1.138405	1.102531	1.077527	1.058814	1.14173	1.087386	1.007394	0.950069	0.9062
C1600-1500	1.23418	1.19021	1.153704	1.106541	1.078284	1.058421	1.146232	1.087587	1.012461	0.957284	0.908684
C2200-300	1.227	1.18971	1.157339	1.109009	1.0728	1.04543	1.149691	1.083716	0.991365	0.926152	0.875618
C2200-700	1.22707	1.18422	1.150066	1.10241	1.067713	1.041053	1.126134	1.068068	0.981325	0.918861	0.870992
C2200-1050	1.29126	1.21673	1.176749	1.120697	1.083117	1.055872	1.204782	1.132402	1.023274	0.946485	0.89101